3rd Specialty Conference on Disaster Prevention and Mitigation
3e Conférence spécialisée sur la prévention et la mitigation des désastres naturels

Montréal, Québec
May 29 to June 1, 2013 / *29 mai au 1 juin 2013*

Sliding Response Analysis of Operational and Functional Components (OFC) in Seismically Isolated Buildings

F. Nikfar, D. Konstantinidis
Department of Civil Engineering, McMaster University

Abstract: Seismic isolation is a practical technique that aims at reducing the damaging effects of earthquakes on structures. Seismic isolation systems have been increasingly developed and implemented over the last three decades, especially for important structures. However, while extensive research has been conducted on investigating the mitigating effects of seismic isolation on the structure itself, very little attention has been paid on the seismic performance of operational and functional components (OFC) in seismically isolated buildings. Sliding of building contents, such as equipment, is of primary concern during an earthquake because not only can it contribute to substantial losses due to equipment damage, but also pose a serious safety risk to building occupants. This paper investigates how seismically isolating a building affects the sliding response of its contents. The contents are idealized as freestanding rigid bodies, free to slide but not rock. The mechanical behaviour of the contact surface between the contents and the building floors is described by a Coulomb friction model. The isolation system is modeled as a linear elastic spring element with a viscous damper. Time history analyses are carried out using the OpenSees dynamic simulation framework, and the sliding response of the contents when placed in seismically isolated versus fixed-base buildings is compared. This study draws the conclusion that in certain cases seismic isolation results in amplification in the peak sliding response of freestanding building contents.

1. Introduction

Damage to critical facilities, such as hospitals, emergency response centers, power plants, substations, key governmental facilities, and important industries may bring about severe human, environmental and economic losses (Politopoulos and Feau 2007). In most of these facilities, the cost and importance of the contents are much more than the structure itself (Yang et al. 2010).

Seismic isolation is a proven technique for reducing the damaging effects of earthquakes on structures (Constantinou et al. 2007, Kelly and Konstantinidis 2011). It achieves this by introducing a horizontally flexible layer at the foundation level which essentially decouples the structure from the motion of the ground. Since its early days, researchers have focused on the effectiveness of seismic isolation in terms of reducing demands on the structure itself, while little attention has been paid to its effect on the performance of Operational and Functional Components (OFC); the rationale being that a reduction in engineering demand parameters that are associated with structural damage will also curtail damage to OFC. More recently, some efforts have been made using floor response spectra towards understanding how different types of base isolation systems affect the performance of attached oscillatory systems (Yang et al. 2010, Isakovic et al. 2011, Politopoulos 2008).

Rocking, sliding and rocking-sliding are response modes of freestanding OFC in an earthquake. Rocking is in principle an undesirable response for OFC because it is very sensitive to the characteristics of the rocking object and input excitation. Small changes in each parameter may contribute to damage or total

loss of the OFC due to impact or overturning (Yim et al. 1980, Makris and Konstantinidis 2003, 2009).

In biological research facilities, equipment often stores very valuable research that can be damaged or destroyed either directly due to the earthquake shaking or indirectly due to malfunction of the equipment (Konstantinidis and Makris 2005, 2009). On the contrary, sliding response is more favorable, although excessive sliding displacements of sensitive/heavy equipment can result in impact with walls or neighbouring OFC, which may endanger the contents or even the equipment itself (Konstantinidis and Makris 2009). Shenton (1996) presented criteria for determining the mode of response of freestanding objects. Slender objects are more prone to rocking, while stocky objects are more prone to sliding. Sliding objects include a wide range of OFC in buildings which are freestanding (i.e., unanchored), either by choice or by necessity. OFC restrained using friction pads also fall under this category.

The problem of sliding objects has been studied in the past at various levels by Shao and Tung (1999), Lopez Garcia and Soong (2003a, b), Hutchinson and Chaudhuri (2006), and Konstantinidis and Makris (2009, 2010). Motivated by Newmark's early solution for the sliding response of mass subjected to a square ground acceleration pulse (Newmark 1965) and using dimensional analysis, Makris and Black (2004) and Makris and Konstantinidis (2005) exposed that the sliding problem exhibits self-similarity under various pulse excitations. For these pulse excitations, the maximum relative displacement U_{max} of the mass, expressed as a dimensionless parameter, is a function Φ of the dimensionless strength of the pulse

$$[1] \qquad \frac{U_{max}}{a_p T_p^2} = \Phi\left(\frac{a_p}{\mu g}\right)$$

where a_p is the pulse acceleration amplitude, T_p is the duration of the pulse, μ is the friction coefficient of the surface, and g is the acceleration of gravity. The function Φ can be obtained either analytically or numerically based on the pulse type. Equation 1 shows that the maximum displacement U_{max} scales with the so-called characteristic length of the excitation, $a_p T_p^2$. For an OFC in a base-isolated building, a_p can be thought of as the floor acceleration amplitude, while T_p can be thought of as the fundamental period of the base-isolated building. Although seismic isolation results in a reduction in a_p, the vibration period T_p is considerably increased, and since the characteristic length scales with the square of T_p, it is possible that the sliding displacements will be amplified if the building is isolated. In reality, an *a priori* conclusion cannot be drawn with certainty because the form of function Φ is not known; any attempt to draw general conclusions is further complicated by the fact that for a random excitation the idea of self-similarity vanishes.

This paper investigates the sliding response of OFC in seismically isolated buildings, aiming to expose situations where isolation may in fact result in response amplification. To this end, a parametric study is carried out to examine the effect of different parameters on the sliding response of the OFC. The seismic performance of sliding OFC in simplified base-isolated and fixed-base structures are compared under two different sets of ground motions (GMs). The first set consists of broad-band GMs and the second of pulse-like GMs, each set comprising twenty records. Linear elastomeric system with supplemental viscous damper assumed as isolation mechanism for the structure. The study shows that, even though implementing seismic isolation in general reduces the response of the structures and its contents, amplification may occur in the sliding response of OFC in certain cases. Therefore, additional measures may be necessary to prevent excessive sliding in seismically isolated buildings. The paper also demonstrates the inherent differences in the seismic response of OFC in seismically isolated buildings subjected to pulse-like and broad-band GMs.

2. Analytical Model

Freestanding rigid objects can have three modes of response during an earthquake (assuming that the object does not lift-off); pure rocking, pure sliding, and rocking-sliding at the same time (Shenton 1996). Shenton presented criteria that determine the dominant response of an object under base excitation.

These include the geometry of the object, the frictional characteristics of the object-floor interface, and the kinematic characteristics of the input motion. This study examines the response of rigid OFC that is stocky enough, and/or for which the friction coefficient is low enough, that the rocking mode is not engaged; and thus pure sliding is the only mode of response. The model used to examine the effect of base isolation on the sliding response of OFC is shown in Figure 1. It consists of three parts: the sliding OFC, the structure, and the base isolation system. Detailed description of each part of this model follows.

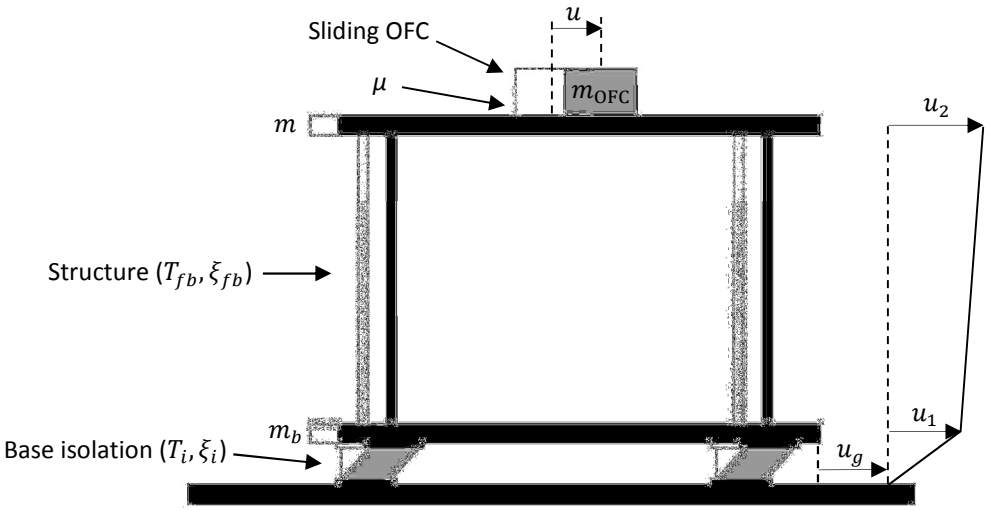

Figure 1: Schematic of the model

2.1 Sliding OFC

A rigid block (i.e., the OFC) of mass $\mathrm{m_{OFC}}$ resting on the second storey is considered, as shown in Figure 2. The dynamic response of the OFC is coupled with the dynamic response of the structural model. However, if the mass of the OFC is very small compared to the mass of the floor, this interaction is negligible. The analysis results presented in this paper neglect this dynamic interaction; in this case, the sliding response of the OFC can be computed separately by using as base input the absolute acceleration of the second storey, i.e., $\ddot{u}_2 + \ddot{u}_g$ in Figure 1, where u_2 is the displacement of the second storey relative to the ground, and $\ddot{u}_g$ is the ground acceleration. u is the displacement of the OFC relative to the second storey, i.e. the *sliding displacement*. The vertical component of the ground motion is neglected in this investigation. However, current studies by the authors suggest that incorporating the vertical component of actual ground motions has little effect on the displacement response of OFC.

Owing to its simplicity, a common idealization of the contact interface between objects is the classical Coulomb friction model, where a static friction coefficient, μ_s, and a kinetic friction coefficient, μ, are used. If $\mu_s = \mu$, then a simple rigid-plastic idealization of the yielding mechanism can be used. This model is employed in the simulations of this study. Validation of this model with shaking table tests has been presented in (Konstantinidis and Makris 2009). In general, although this model has resulted in a fair prediction of the shaking table tests (Konstantinidis and Makris 2009), it was considered to be a good representative of the mean response under a set of ground motions (Chaudhuri and Hutchinson 2006). Moreover, based on previous studies (Chaudhuri and Hutchinson 2006, Konstantinidis and Makris 2009), variation of the coefficient of static friction, μ_s, has little influence on the maximum sliding displacement of the OFC. On the contrary, the maximum sliding displacement is sensitive to the kinetic coefficient of friction, μ. An improved prediction of shake table results can be achieved by taking into account the pressure- and velocity-dependence of the kinetic coefficient of friction; however, such an elaborate friction model is beyond the scope of this paper.

In the case of pure sliding, the OFC will start sliding once the base acceleration overcomes the frictional resistance of the interface. This is prescribed by the condition

[2] $$\left|\ddot{u}_2 + \ddot{u}_g\right| > \mu_s g$$

where g is the acceleration of gravity. The equation of motion for the sliding displacement of the OFC, u, is

[3] $$\ddot{u} + \mu g \ \mathrm{sgn}\left(\dot{u}\right) = -\left(\ddot{u}_2 + \ddot{u}_g\right)$$

where $\mathrm{sgn}(\cdot)$ is the *signum* function. If $\dot{u}$ becomes zero, and the condition prescribed by Eq. 2 is not satisfied, then the block sticks to the floor. The seismic response can be determined by solving Eq. 3, where the input excitation $-(\ddot{u}_2 + \ddot{u}_g)$ is obtained by first conducting time history analysis of the model shown in Figure 1 without the OFC.

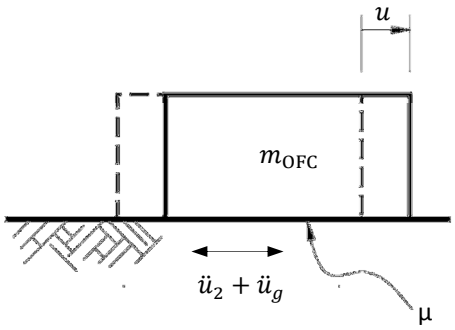

Figure 2: Free-body-diagram of the slider block

The dynamic simulation software framework OpenSees (Mazzoni et al. 2007) is used to simulate the sliding OFC. The friction mechanism at the interface between the OFC and the floor is modeled using a *Flat Slider Bearing Element* (developed by A. Schellenberg). To validate the OpenSees Flat Slider Bearing Element, the results of dynamic simulations in OpenSees using this element were compared with the results of solving Eq. 3 in MATLAB (2002) using the ODE45 solver. Figure 3 shows the sliding response of an OFC with $\mu = 0.1$ subjected to the floor motion resulting from the JAMA record of the 1995 Kobe earthquake. The results of the OpenSees and MATLAB simulations are in excellent agreement with each other. The very slight discrepancy between the two is attributed to the order of the solvers. OpenSees utilizes Newmark's 2nd-order method to solve the equation, while the MATLAB ODE45 solver uses fourth and fifth order Runge-Kutta formulas.

2.2 Structure Model and Base Isolation System

An elastic single degree of freedom shear structure, as shown in Figure 1, is considered as the superstructure mounted on a fixed- or an isolated base. The mass of the superstructure and foundation are assumed to be identical ($m = m_b$), and 2% damping is considered for the superstructure. A viscously damped linear elastic isolation system is assumed in this study. This model was used from early on to introduce the linear theory of seismic isolation (Kelly 1996). This simple model is very convenient for parametric studies. The overall force-displacement response of the system can be obtained by superposition of the behaviour of constitutive elements. Utilizing this model, the nominal period and damping of the isolation system are given by (Kelly 1996)

[4] $$T_i = 2\pi\sqrt{\frac{m+m_b}{k_i}}$$

[5] $$\xi_i = \frac{c_i T_i}{4\pi(m+m_b)}$$

where T_i and ξ_i are the nominal period and nominal damping ratio of the isolated structure and k_i, and c_i are the stiffness and damping coefficients of the isolation. The definitions for the nominal period and damping ratio of the isolated structure given by Equations 4 and 5, are based on the premise that in a seismically isolated building, the superstructure moves as a nearly rigid body. In reality, the fundamental period of the system is slightly larger than the nominal period.

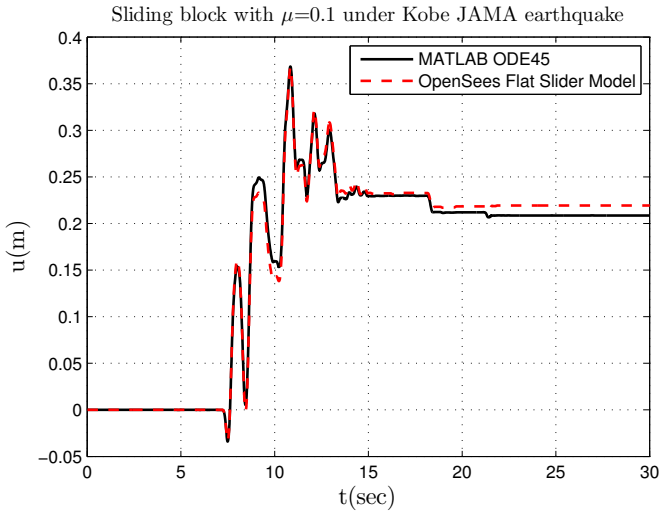

Figure 3: OFC sliding displacement obtained using the OpenSees Flat Slider Element and MATLAB ODE solver

3. Selection of Ground Motions

The seismic response of the sliding OFC in base-isolated buildings investigated in this study is based on two sets of input ground motions: (a) a set of 20 broad-band motions, and (b) a set of 20 pulse-like motions. The ground motions used are selected randomly from standardized sets of ground motions provided in Baker et al. (2011). These standardized ground motion sets were developed such that the mean and variance of their logarithmic response spectra match that predicted for a 'generic earthquake scenario' typical of high seismicity sites in California (Baker et al. 2011). Description of the ground motions are summarized in Table 1. More details can be found in Baker et al. (2011).

4. Dynamic Analysis Procedure

To examine the effect of using seismic isolation on sliding performance of OFC, a series of non-linear time-history analyses were performed on the previously defined model. For simplicity, only the horizontal component of the ground motions is considered. The mean of the peak OFC sliding displacements and the mean of the peak OFC absolute accelerations in the horizontal direction are considered the engineering demand parameters (EDPs) of interest in this parametric study. The effect of the seismic isolation design parameters T_i and ξ_i on the performance of the OFC, as quantified by the chosen EDPs, was examined. The effectiveness of seismic isolation on the sliding displacement is clearly demonstrated by means of presenting the ratio of the mean maximum displacement of the OFC in the isolated structure, $\overline{U}_i$, to corresponding mean maximum displacement of the OFC in a fixed-base structure, $\overline{U}_{fb}$.

Table 1: Broad-band and pulse-like ground motions used in this study

Broad-Band set			Pulse-Like set		
Earthquake Name	Station	Filename in Database (Baker et al. 2011)	Earthquake Name	Station	Filename in Database (Baker et al. 2011)
Mammoth Lakes-01/1980	'Long Valley Dam (Upr L Abut)	'M7_soil_FN_1.acc'	Imperial Valley-06/1979	EC Meloland Overpass FF	'PL_2_SN.acc'
Cape Mendocino/1992	Rio Dell Overpass - FF	'M7_soil_FN_3.acc'	Imperial Valley-06/1979	El Centro Array #4	'PL_3_SN.acc'
Kocaeli, Turkey/1999	Yarimca	'M7_soil_FP_5.acc'	Imperial Valley-06/1979	El Centro Array #5	'PL_4_SN.acc'
Chi-Chi, Taiwan/1999	NST	'M7_soil_FP_8.acc'	Imperial Valley-06/1979	El Centro Array #6	'PL_5_SN.acc'
Kocaeli, Turkey/1999	Duzce	'M7_soil_FP_9.acc'	Imperial Valley-06/1979	El Centro Array #7	'PL_6_SN.acc'
Loma Prieta/1989	Gilroy Array #4	'M7_soil_FN_12.acc'	Imperial Valley-06/1979	El Centro Array #8	'PL_7_SN.acc'
Loma Prieta/1989	Fremont - Emerson Court	'M7_soil_FP_15.acc'	Imperial Valley-06/1979	El Centro Differential Array	'PL_8_SN.acc'
Chalfant Valley-02/1986	Zack Brothers Ranch	'M7_soil_FP_16.acc'	Morgan Hill/1984	Coyote Lake Dam (SW Abut)	'PL_9_SP.acc'
Imperial Valley-06/1979	El Centro Array #4	'M7_soil_FN_19.acc'	Loma Prieta/1989	LGPC	'PL_11_SN.acc'
Landers/1992	Yermo Fire Station	'M7_soil_FP_21.acc'	Landers/1992	Lucerne	'PL_12_SN.acc'
San Fernando/1971	LA - Hollywood Stor FF	'M7_soil_FN_23.acc'	Northridge-01/1994	Jensen Filter Plant	'PL_14_SN.acc'
N. Palm Springs/1986	Morongo Valley	'M7_soil_FP_24.acc'	Northridge-01/1994	Newhall - W Pico Canyon Rd.	'PL_17_SN.acc'
Loma Prieta/1989	Hollister - South & Pine	'M7_soil_FN_25.acc'	Northridge-01	Rinaldi Receiving Sta	'PL_18_SN.acc'
Chi-Chi, Taiwan/1999	CHY025	'M7_soil_FN_27.acc'	Northridge-01/1994	Sylmar - Converter Sta	'PL_19_SN.acc'
Imperial Valley-06/1979	Brawley Airport	'M7_soil_FN_28.acc'	Northridge-01/1994	Sylmar - Olive View Med FF	'PL_21_SN.acc'
Duzce, Turkey/1999	Duzce	'M7_soil_FN_30.acc'	Kobe, Japan/1995	KJMA	'PL_22_SN.acc'
Chi-Chi, Taiwan/1999	TCU061	'M7_soil_FP_31.acc'	Chi-Chi, Taiwan/1999	CHY101	'PL_26_SP.acc'
Loma Prieta/1989	Saratoga - Aloha Ave	'M7_soil_FN_32.acc'	Chi-Chi, Taiwan/1999	TCU052	'PL_28_SN.acc'
Imperial Valley-02/1940	El Centro Array #9	'M7_soil_FN_33.acc'	Chi-Chi, Taiwan/1999	TCU068	'PL_31_SP.acc'
Loma Prieta/1989	Coyote Lake Dam (Downst)	'M7_soil_FP_38.acc'	Chi-Chi, Taiwan/1999	TCU076	'PL_33_SN.acc'

To examine the OFC sliding behaviour for a wide range of possible OFC-floor frictional resistance, analyses were conducted varying the friction coefficient from $\mu = 0.05$, which can be thought for portable OFCs on wheels, to $\mu = 0.8$, which in practice is relatively a large value.

5. Effect of Seismic Isolation on OFC Performance

The effect of seismic isolation on the performance of OFC is examined by means of conducting a parametric study and presenting the response in terms of EDPs under two different sets of GMs.

5.1 Peak Relative Displacement Demand

For a base isolated structure with fixed T_i, T_{fb}, ξ_i, ξ_{fb}, and μ, the mean of the maximum OFC sliding displacements from the twenty records was computed, $\overline{U}_i$. To evaluate the effect of base isolation on the sliding displacement response, this mean value is divided by the mean of the maximum OFC sliding displacements in a fixed-base structure with the same T_{fb}, ξ_{fb}, and μ. The ratio, $\overline{U}_i/\overline{U}_{fb}$, represents how

seismic isolation affects maximum relative displacement of the OFC. Figure 4 shows sliding relative displacement ratio for various isolation periods, T_i, and kinetic friction coefficients, μ.

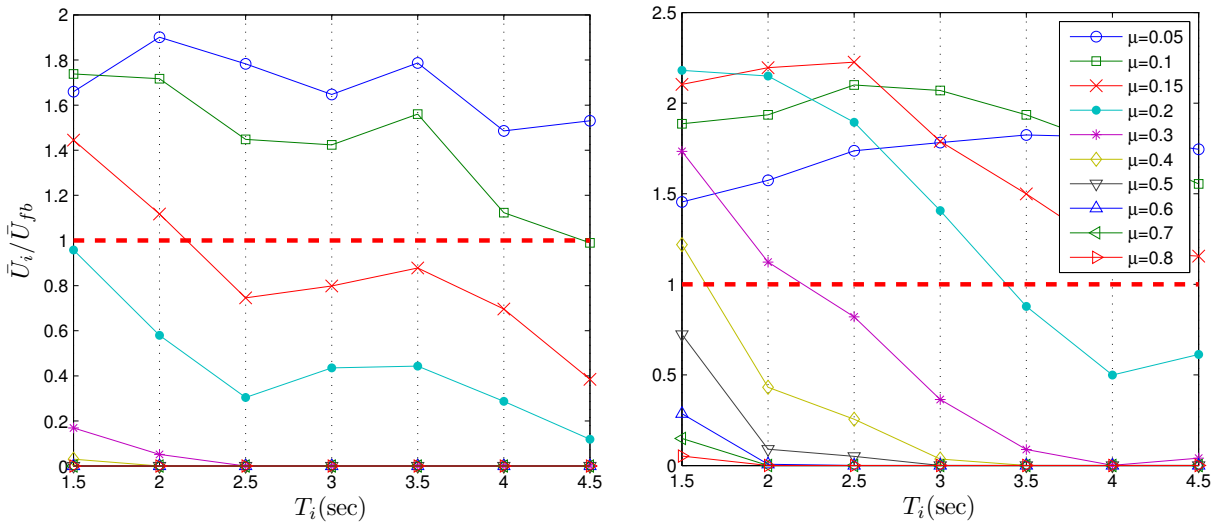

Figure 4: OFC sliding displacement ratio as a function of isolation period T_i. Left: Broad-Band GM. Right: Pulse-Like GM ($\xi_i = 10\%$, $T_{fb} = 0.2$ sec)

The dashed line denotes the case when the sliding OFC in the seismically isolated and the fixed-base buildings experience the same maximum relative displacement. The points above this line indicate that seismically isolating the building results in amplification in OFC displacement response. The figure shows that there are a number of combinations of T_i and μ for which seismic isolation results in amplification of OFC sliding displacements. According to Figure 4(left), under broad-band ground motions, freestanding OFC items with coefficient of friction less than 0.15 are likely to experience sliding displacements that are greater if the building is isolated than if the building is fixed-base. Increasing the isolation period from 1.5 sec to 2.5 sec, the curve corresponding to $\mu = 0.15$ drops below 1.0; however, further increase in T_i results in an increase in maximum displacement ratio. Therefore, increasing the isolation period not always leads to decrease in the OFC sliding displacement response. Based on the curves in Figure 4, amplification in OFC sliding displacements in base-isolated buildings is more likely for lower friction coefficients. Figure 4(right), presents the variation of displacement ratio under pulse-like ground motions. It can be seen that unlike broad-band GMs, for low μ the ratio is not following a certain trend. However, beyond a certain μ value, here 0.3, implementing seismic isolation with $T_i > 2.2$ sec results in OFC sliding displacements that are lower than in the corresponding fixed-base structure.

Under both sets of GMs, the OFC displacement response can be decreased by introducing more damping at the isolation level, as shown in Figure 5. As can be seen, an increase in ξ_i results in a decrease in relative displacement, but its effect varies after a specific point. The effectiveness of damping also varies with μ. For instance, increasing ξ_i to values more than 15% in the case of $\mu = 0.2$ has little effect on the rate of decrease in the sliding displacement ratio. However, providing a small amount of damping can be very effective in this respect.

5.2 Peak Absolute Acceleration Demand

The maximum absolute acceleration that the OFC experience is the other engineering demand parameter considered in this study. The ratio of the mean of the maximum absolute accelerations is presented in Figure 6. In this figure, the variation of maximum absolute acceleration ratio is shown for different T_i and μ. As can be seen in Figure 6(left), under broad-band GMs, utilizing seismic isolation considerably decreases the absolute acceleration response of the contents. However, under pulse-like GMs, no

specific trend can be identified in the maximum acceleration response ratio of OFC with low friction coefficient (Figure 6-right).

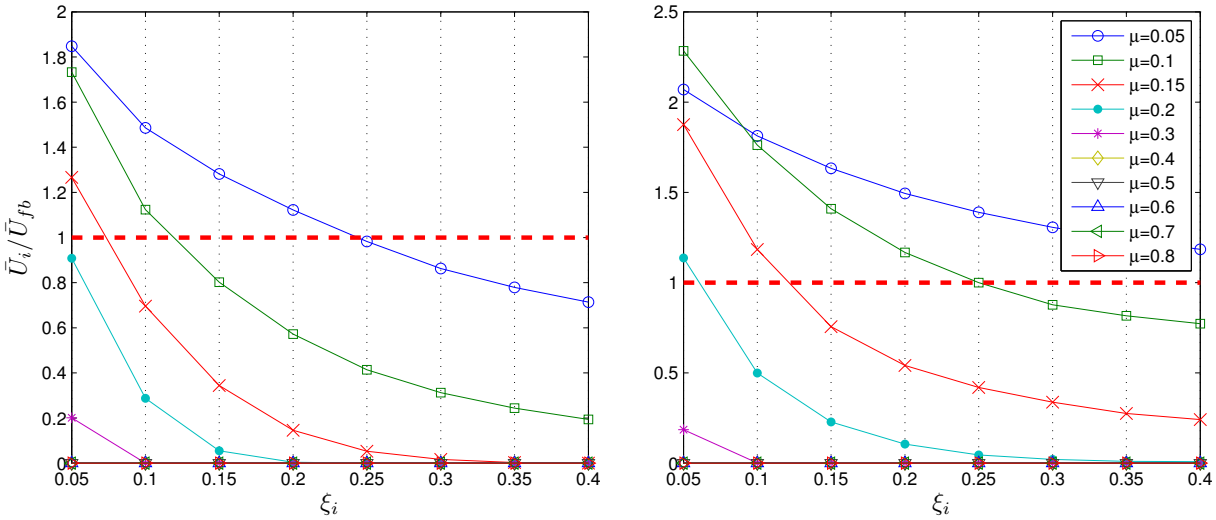

Figure 5: OFC sliding displacement ratio as a function of isolation damping ratio ξ_i. Left: Broad-Band GM. Right: Pulse-Like GM ($T_i = 4.0$ sec, $T_{fb} = 0.2$ sec)

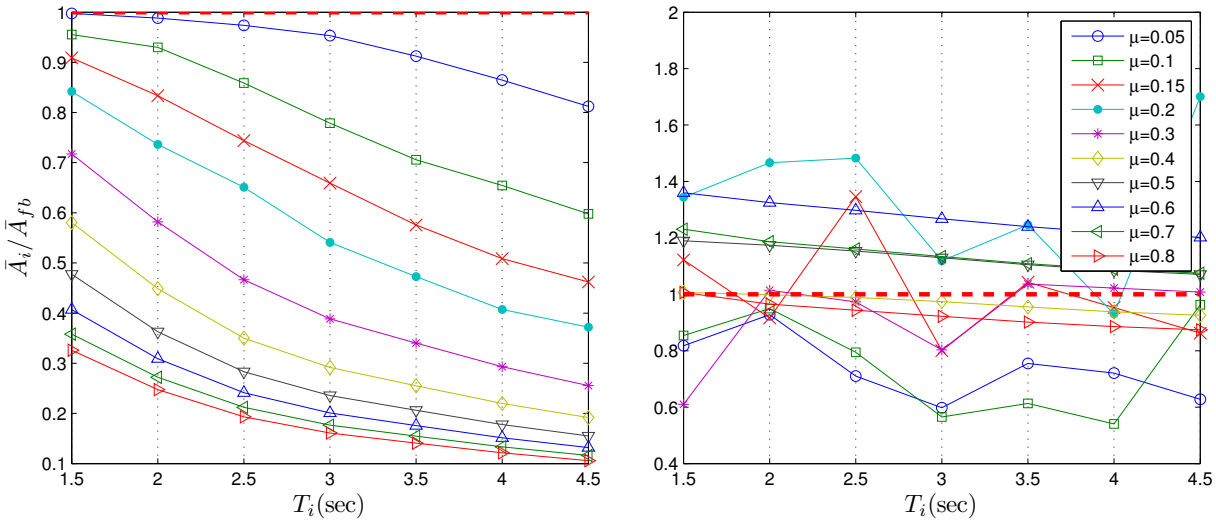

Figure 6: OFC absolute acceleration ratio as a function of T_i. Left: Broad-Band GM. Right: Pulse-Like GM ($\xi_i = 10\%$, $T_{fb} = 0.2$ sec)

Since the characteristics of pulse-like ground motions are entirely different than those of broad-band ground motions, it is possible that an order may emerge if a more sophisticated intensity measure is used. The choice of such an intensity measure is currently under investigation.

The effect of isolation damping on the OFC absolute acceleration is illustrated in Figure 7. Under broad-band GMs, increasing the isolation damping results in reduced OFC acceleration response (Figure 7-left). Like for OFC sliding displacement, increasing ξ_i after a specific value, in this case about 20%, shows no effect on the response. Moreover, the effectiveness of supplementary damping in reducing OFC

accelerations depends on μ. Contrary to broad-band GMs, Figure 7(right) shows that for pulse-like motions, the maximum acceleration response ratio does not follow an identifiable trend with increasing ξ_i.

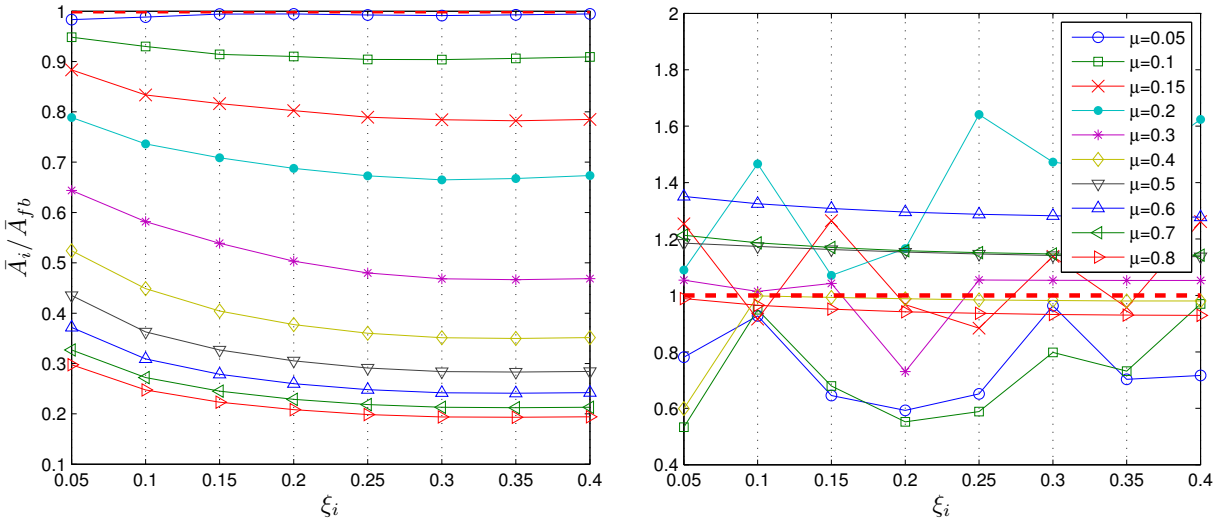

Figure 7: OFC absolute acceleration ratio, ξ_i is changing. Left: Broad-Band GM. Right: Pulse-Like GM ($T_i = 2.0$ sec, $T_{fb} = 0.2$ sec)

6. Conclusions

This paper examines the seismic response of operational and functional components (OFC) that are prone to sliding in seismically isolated structures. A parametric study has been conducted in order to investigate the effect of the isolation period and damping ratio on the sliding displacements and absolute accelerations of sliding OFC under two sets of ground motions: a set of broad-band motions and a set of pulse-like motions. Ground motions are selected from sets of recommended ground motions recently developed by Baker et al. (2011). The OpenSees dynamic simulation software framework is utilized to simulate the OFC and base-isolated building. Since the mass of the OFC is considered to be low compared the floor mass, it is assumed that the dynamic interaction between the OFC and the building is negligible; this allows the dynamic response of the OFC to be computed by using as base input the floor acceleration computed from dynamic analysis of the base isolated building. The model is validated against the "exact" solution obtained by integrating the equation of motion using standard ODE solvers in MATLAB. This parametric study considers only the horizontal component of the ground motions. The results are presented as ratios of the mean of the maximum responses in the base isolated building versus the fixed-base building. It is observed that there are a number of combinations of isolation period, isolation damping and OFC friction coefficient, for which implementing seismic isolation can contribute to amplification in sliding displacements compared to the fixed-base structure. This amplification is more likely in lower friction coefficients. It is also shown that providing a minimum amount of damping at the isolation level will work effectively in decreasing the sliding displacements. However, additional damping (here, more than 20%) has little effect on the displacement response. Under broad-band GMs, application of seismic isolation considerably decreases the absolute acceleration response of sliding OFC. In contrast, acceleration response of the OFC does not follow an identifiable trend under pulse-like GMs.

7. References

Baker, J.W., Lin, T., Shahi, S.K. & Nirmal, J., 2011. *New Ground Motion Selection Procedures and Selected Motions for the PEER Transportation Research Program*. PEER 2011/03. Pacific Earthquake Engineering Research Center.

Chaudhuri, S.R. & Hutchinson, T.C., 2006. Fragility of Bench-Mounted Equipment Considering Uncertain Parameters. *Journal of Structural Engineering*, 132(6), p.884–898.

Constantinou, M.C. et al., 2007. *Performance of seismic isolation hardware under service and seismic loading*. MCEER-07-0012. Buffalo: Multidisciplinary Center for Earthquake Engineering Research State University of New York.

Garcia, L.D. & Soong, T.T., 2003. Sliding fragility of block-type non-structural components. Part 1: unrestrained components. *Earthquake Engineering and Structural Dynamics*, 32(1), p.111–129.

Garcia, L. & Soong, T., 2003. Sliding fragility of block-type non-structural components. Part 2: restrained components. *Earthquake Engineering and Structural Dynamics*, 32(1), p.131–149.

Hutchinson, T.C. & Chaudhuri, R., 2006. Bench-shelf system dynamic characteristics and their effects on equipment and contents. *Earthquake Engineering and Structural Dynamics*, 35(13), p.1631–1651.

Isakovic, T., Zevnik, J. & Fischinge, M., 2011. Floor response spectra in isolated structures subjected to earthquakes weaker than the design earthquake—Part I: Isolation with high-damping rubber bearings. *Structural Control and Health Monitoring*, 18, p.635–659.

Kelly, J.M., 1996. *Earthquake Resistant Design with Rubber*. 2nd ed. New York, NY: Springer.

Kelly, J.M. & Konstantinidis, D., 2011. *Mechanics of Rubber Bearings for Seismic and Vibration Isolation*. Chichester, UK: John Wiley & Sons.

Konstantinidis, D. & Makris, N., 2009. Experimental and analytical studies on the response of freestanding laboratory equipment to earthquake shaking. *Earthquake Engineering and Structural Dynamics*, 38, p.827–848.

Konstantinidis, D. & Makris, N., 2010. Experimental and analytical studies on the response of 1/4-scale models of freestanding laboratory equipment subjected to strong earthquake shaking. *Bulletin of Earthquake Engineering*, 8, p.1457–1477.

Konstantinidis, D. & Markis, N., 2005. *Experimental and Analytical Studies on the Seismic Response of Freestanding and Anchored Laboratory Equipment*. PEER 2005/07. University of California, Berkeley.

Makris, N. & Black, C.J., 2004. Dimensional Analysis of Rigid-Plastic and Elastoplastic Structures under Pulse-Type Excitations. *Journal of Engineering Mechanics*, 130(9), p.1006–1018.

Makris, N. & Konstantinidis, D., 2003. The Rocking Spectrum and the Limitations of Practical Design Methodologies. *Earthquake Engineering and Structural Dynamics*, 32(2), p.265–289.

MATLAB, 2002. *High-performance Language Software for Technical Computing*. The MathWorks, Inc.: Natick, MA.

Mazzoni, S., McKenna, F., Scott, H. & Fenves, G., 2007. *Open System for Earthquake Engineering Simulation (OpenSees) Command Language Manual*. (http://opensees.berkeley.edu).

Newmark, N.M., 1965. Effects of earthquakes on dams and embankments. *Géotechnique*, 15, p.139–160.

Politopoulos, I. & Feau, C., 2007. Some aspects of floor spectra of 1DOF nonlinear primary structures. *Earthquake Engineering and Structural Dynamics*, 36, p.975–993.

Politopoulos, I., 2008. A review of adverse effects of damping in seismic isolation. *Earthquake Engineering and Structural Dynamics*, 37, p.447–465.

Shao, Y. & Tung, C., 1999. Seismic response of unanchored bodies. *Earthquake Spectra*, 15(3), p.523–536.

Shenton, H.W., 1996. Criteria for Initiation of Slide, Rock, and Slide-Rock Rigid-Body Modes. *Journal of Engineering Mechanics*, 122(7), p.690–693.

Yang, T.Y., Konstantinidis, D. & Kelly, M., 2010. The Influence of Isolator Hysteresis on Equipment Performance in Seismic Isolated Buildings. *Earthquake Spectra*, 26(1), p.275–293.

Yim, S.C.S., Chopra, A.K. & Penzien, J., 1980. Rocking Response of Rigid Blocks to Earthquakes. *Earthquake Engineering and Structural Dynamics*, 8(6), p.565–587.